Available online at www.sciencedirect.com

jmr&t Journal of Materials Research and Technology

www.jmrt.com.br

Original Article

Eddy current and inspection of coatings for storage tanks☆

Marcella Grosso[a,b,*], *Clara J. Pacheco*[b], *Mónica P. Arenas*[a,b], *Andre H. Mascarenhas Lima*[b], *Isabel C.P. Margarit-Mattos*[a,b], *Sergio Damasceno Soares*[c], *Gabriela R. Pereira*[a,b]

[a] *Department of Metallurgical and Materials Engineering, Federal University of Rio de Janeiro (UFRJ), Polytechnic School and COPPE, 21941-972 Rio de Janeiro, RJ, Brazil*

[b] *Laboratory of Nondestructive Testing, Corrosion and Welding (LNDC), Department of Metallurgical and Materials Engineering, Federal University of Rio de Janeiro (UFRJ), Polytechnic School and COPPE, 21941-596 Rio de Janeiro, RJ, Brazil*

[c] *Petrobras Research Center (CENPES), 21040-000 Rio de Janeiro, RJ, Brazil*

ARTICLE INFO

Article history:
Received 17 November 2017
Accepted 2 May 2018
Available online 30 June 2018

Keywords:
Eddy current testing
Coatings
Corrosion
Underfilm corrosion
Pitting

ABSTRACT

The aim of this work is to make a survey of typical flaws presented by modern anticorrosive coatings commonly employed for inside protection of petrochemicals storage tanks and discuss what can be expected from nondestructive inspection with conventional eddy current technique. In this sense, advantages and limitations of the method are discussed taking into account the characteristics of the coatings. Controlled defects were machined in carbon steel substrates in order to simulate localized corrosion. The detectability of the eddy current technique was evaluated for as-applied insulating coatings (with different thicknesses) in presence and absence of iron oxide inside the simulated corrosion defects. Comparing the results obtained with the original C-Scan maps and after the image processing, the machined defects were successfully detected. In this comparison, it was observed a significant improvement for the false defects elimination using image processing.

1. Introduction

Coatings have been widely applied for the protection of metallic substrates against corrosion [1]. Throughout the last decades, the employment of anticorrosive composite coatings has been considered as an attractive option for industrial plants operating under severe environmental conditions, such as high temperatures, sour service and mechanical stress by different agents [2,3]. The use of anticorrosive composites is one of the several existing methods to control corrosion, which has gained extensive application particularly in oil and gas industry, and are usually found in storage tanks, pipelines, heat exchangers, and structural components.

☆ Paper was part of technical contributions presented in the events part of the ABM Week 2017, October 2nd to 6th, 2017, São Paulo, SP, Brazil.

* *Corresponding author.*
E-mail: marcellag@metalmat.ufrj.br (M. Grosso).

https://doi.org/10.1016/j.jmrt.2018.05.006

Table 1 – Characteristics of the samples.

Sample	Coating	Dry coating thickness (μm)	Corrosion product	Defect diameter (mm)					
				1	2	3	4	5	6
A	EP	972 ± 55	No	5.45	5.25	5.25	10.75	11.00	10.84
B	EA	376 ± 60	No	5.41	5.36	5.26	11.20	11.20	11.24
C	EP	582 ± 125	Yes	5.65	5.56	5.53			
D	EP	670 ± 140	Yes	4.89	4.98	4.64			

Inspection is required because the coatings can present blistering, lack of adherence and undercoating corrosion. Such failures may occur due to incorrect application procedures, but also are inherent to coatings ageing. In this context, the use of non-destructive techniques (NDTs) is justified by the subjectivity in visual assessments, in which the detection of interlayer and/or undercoating flaws are of difficult access. Therefore, magnetic NDTs allow inspection after the coating application, ensuring application efficiency, as well as monitoring periodically the coating performance and the evolution of its integrity in service.

The eddy current testing (ECT) is based on the interaction between the primary magnetic field and the tested material. This interaction induces eddy currents within the test piece [4]. The presence of discontinuities, such as corrosion and material losses, are detected by monitoring the coil impedance changes or by measuring the induced magnetic field [4,5]. Conventional ECT operates in a single frequency, in which the excitation coil is driven by a sinusoidal wave [6]. In case of non-conductive composites, this technique may have limitations with the depth of penetration, since the lift-off affects the signal-to-noise ratio [7,8]. However, mathematical models may be implemented in order to consider lift-off variations or even neglecting the lift-off effect in the impedance plane [4,9–13]. Thus, the purpose of this study is to analyze the performance of ECT for detection of localized corrosion in carbon steel substrates coated with commercial coatings, which are commonly used in petrochemical storage tanks.

2. Materials and experiment procedures

The experimental included preparation of samples with controlled defects and non-destructive inspection using ECT and data processing.

2.1. Coatings

Two commercial coatings were chosen for this study: (i) a two components epoxy phenolic coating reinforced with glass flakes and low volatile organic content (EP), and (ii) a 100% solids, thin film coating of modified epoxy resin reacted with a modified cycloaliphatic amine reinforced with proprietary blend of modified mineral (EA).

2.2. Samples

Plain carbon steel samples were manufactured in order to characterize the presence of defects by ECT. The samples were made of carbon steel with dimensions of 150 mm × 100 mm × 4.7 mm, coated with anti-corrosive coating. The surface preparation consisted of degreasing and blasting with glass microspheres until white metal. Before applying the coatings, holes were machined with different diameters on the substrate. Some holes were fulfilled with iron oxide (Fe_3O_4) in order to simulate localized corrosion with the presence of undercoating solid corrosion products. The application of the coating consisted of two steps. Firstly, a thin layer of the coating was applied by brush on the surface of the metal substrate avoiding the area of the holes. Before drying, this thin layer of the coating itself worked as an adhesive for free films of the same coating, which were previously prepared. The free films were prepared on a Teflon plate with an extender. Once dried, the films were detached manually from the Teflon plates and glued on the surface of the testing samples with the coating thin layer still humid. Complete description of the samples with machined defects is in Table 1. The samples A and B were fabricated with different coatings in order to evaluate if this variable influences on the defects detection. Samples C and D were painted with EP, with different thicknesses and iron oxide inside the holes. The purpose was to evaluate the detection limit of the technique in presence of corrosion product. The coatings dry thicknesses were measured at twenty different points on each sample with Elcometer 456 equipment. The mean values with mean deviation for each type of sample are shown in Table 1.

2.3. Eddy current testing

Coating thickness heterogeneities affect the eddy current signals due to lift-off variations [9,10,14]. In classical ECT, where the complex impedance plane is used, there is a simple solution for the lift-off cancellation, which is the phase rotation of the signal [11]. The complex impedance plane contains resistance (R) and inductive reactance (X_L) components. The total electrical impedance and phase angle are calculated using Eqs. (1) and (2), respectively [4].

$$Z = \sqrt{R^2 + X_L^2} \tag{1}$$

$$\tan\varphi = \frac{X_L}{R} \tag{2}$$

In this study, the complex impedance plane was rotated in order to constrain the lift-off signal on the vertical axis (Y-axis) and the crack/defect signal on the horizontal (X-axis). Thus, after the rotation, C-Scan maps were built with the real part of the impedance plane, it means, with the resistance component that contains the defect information. The maps are built with the resistance component, which can present

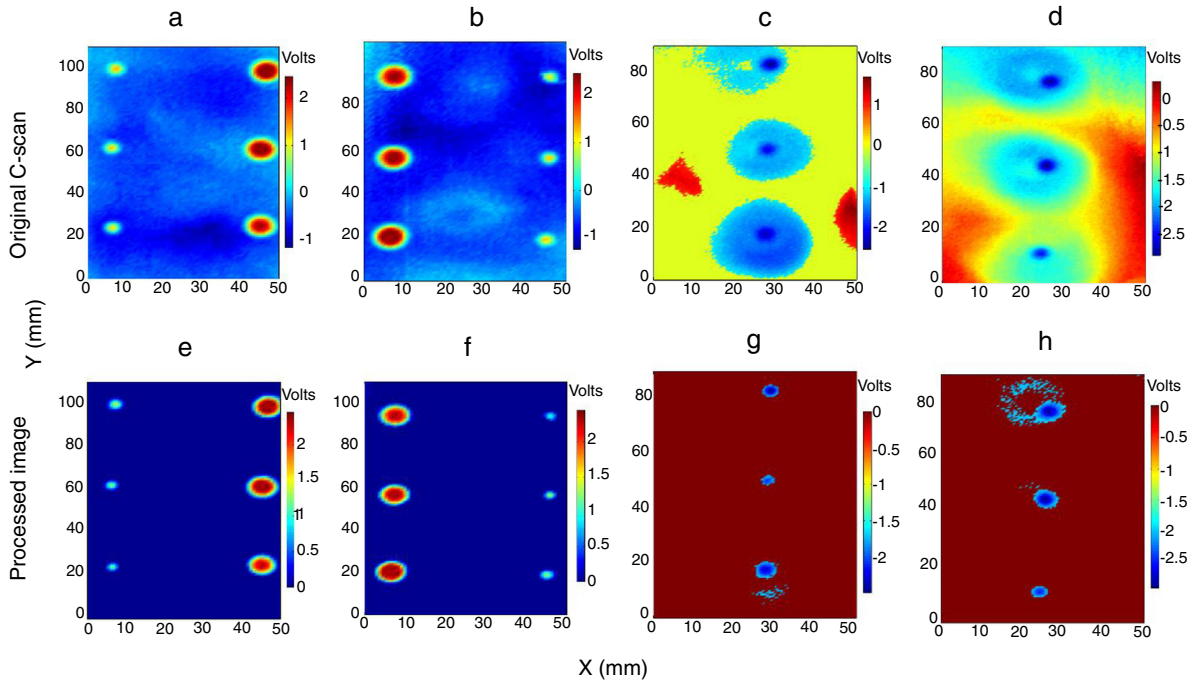

Fig. 1 – Original C-scan map: (a) sample A coated with EP 972 ± 55 μm; (b) sample B coated with EA 376 ± 60 μm; (c) sample C coated with EP 582 ± 125 μm; (d) sample D coated with EP 670 ± 140 μm. Processed image of samples: (e) A; (f) B; (g) C; (h) D.

positive or negative values. Even using this procedure, there is still an influence of the lift-off effect due to the coating thickness variation (Table 1), as will be observed in the original C-scan images. The data were stored in matrices for plotting the C-scan maps and for the image processing. The experimental set-up consisted of eddy currents ZETEC equipment – MIZ 21, probe ZETEC – 5–50 kHz; oscilloscope Tektronix MSO 4034; software developed in LABVIEW for signal acquisition, data analysis and control the XYZ scanning system. As the data acquisition was performed by using an oscilloscope, the resistance component was extracted in volts instead of ohms. The signals were acquired when scanning the sample in x and y with resolution of 1 mm per step. The impedance plane calibration was done in a region without machined defects, near the border of each sample. This region was set as the point (0,0) in the XY coordinate system. As shown in Table 1, sample A presents the highest coating thickness. Thus, in this sample was estimated the penetration depth (δ) by using CIVA software. When the frequency was set at 10 kHz, the δ on this sample was approx. 1.4 mm. Even the eddy currents presenting a depth of penetration on the carbon steel substrate around 0.5 mm, the defects were detected since the inspection was performed on the same side of the defects. At this depth, the eddy current signals presented a high signal-to-noise ratio, which allowed to detect the defects shape satisfactorily.

2.4. *Image processing*

The C-scan scale depends on the values of the analyzed signal, which were peculiar to each sample. The multilevel threshold for image processing was used in order to highlight the corrosion defects and to eliminate false defects, caused by lift-off [15,16]. Mathematically, the multilevel threshold processing creates a processed image $g(x)$, changing the intensity of the grey scale of the original image $f(x)$. The processed image is not binarized making possible to isolate and to distinguish several objects from the bottom [17]. This process required the choice of a primary threshold (t), preferably in a region near the edge of the holes. The values of secondary thresholds would be equal to the value of the initial element of the image, aiming at eliminating regions of false defects in the original image and enabling differentiation after processing. Signals of defects may be positives or negatives, depending on sensor calibration [18,19]. The criterion used to eliminate the presence of false defects and improve the detectability was considering that if defects have positive resistance values, Eqs. (3a) and (3b) would be used for the image processing. But, if the defects present negative resistance values, Eqs. (3c) and (3d) would be used. This criterion ensures that regions with resistance values different from zero are those having real defects. The resistance values also may change depending on the defect. The size of the defects was performed on the original images. The brush tool of Matlab was used to calculate the arithmetic average of the diagonal in x and y-axis of the defects.

$$\begin{aligned} &g(x,y) = f(x,y) \text{ if } f(x,y) \geq t \quad \text{(a)} \\ &0 \text{ if } f(x,y) < t \quad \text{(b)} \\ &g(x,y) = f(x,y) \text{ if } f(x,y) \leq t \quad \text{(c)} \\ &0 \text{ if } f(x,y) > t \quad \text{(d)} \end{aligned} \tag{3}$$

3. Results

3.1. *Defects detection*

As described in Section 2.3, the C-scan maps are built with the resistance component of the impedance plane. In Fig. 1a–d there are the original C-scan images for samples A-D. The scanning was performed on the same side of the machined defects. The ECT method was able to detect all defects in samples A-D, even in those defects filled with corrosion product (Fe_3O_4). In order to neglect the thickness variation, caused by coating heterogeneities, the multilevel thresholding was used for the image processing, Fig. 1e–h.

Samples A and B have resistance values around 2.5 V for defects with larger diameters and those with smaller diameters presented values of approx. 1.5 V, as shown on original C-scan maps, Fig. 1a and b. Negative resistance values are associated with the response on regions with no defects. There is also negative resistance values with lower magnitude related to the coating thickness variations. As described in Section 2.4, the multilevel thresholding was used for eliminating the thickness variation effect and also to improve the defects detectability, increasing the contrast and definition, as shown in Fig. 1e–f. Still in Fig. 1, defects in the original image of samples C and D showed negative resistance values of approximately −2.5 V, Fig. 1c and d. There are regions around the defects with also negative resistance values and lower magnitude. These regions are associated with adhesion failure between the coating and the substrate. Though, there are regions with positive resistance values (in red) caused by the variation of the coating thickness, this signal may be related to false defects. Defects in both samples contain corrosion product and all of them were detected with the eddy current method. After the image processing, it is observed that lift-off variation was considerably reduced, highlighting the real defects, Fig. 1g–h.

According to these results, it was observed that the ECT is a method able to detect the presence of defects, which simulate localized corrosion, in carbon steel substrates. The image processing allowed highlighting the region of interest and eliminating the false defects caused by coating thickness variation.

3.2. *Defect sizing on the original C-scan image*

The dimensioning of the defects was performed using the brush tool of Matlab, which allows calculating the arithmetic average of the diagonal in *x* and *y*-axis of the defects. Fig. 2 shows the defects sizing performed on the original C-scan images of samples A-D. For sample A, the error bars indicate a maximum relative error of 5% in defect 2 with nominal diameter of approx. 5 mm. For sample B, the maximum relative error of approximately 7% was observed for defect 6 with 11.24 mm diameter. Comparing the error bars for defects in samples A (972 ± 55) and B (376 ± 60), it can be concluded that nor the defect diameter, neither the coatings thicknesses have influence on the method accuracy.

Still in Fig. 2, the coating on samples C and D is the same EP as on sample A, but with lower thicknesses, and there is iron oxide inside the defects. The relative error of the defects diameter calculation in these samples varies from 2% to 12%. These errors are in the same range of samples A and B, suggesting that corrosion products do not influence the method accuracy and confirming that it does not depend on this thickness variation.

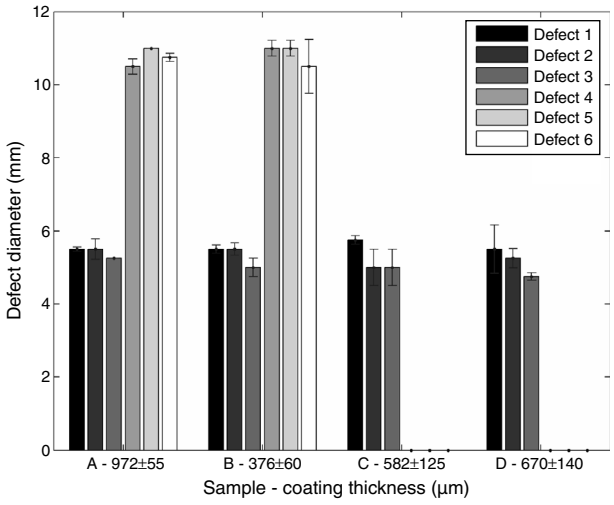

Fig. 2 – Defect dimensions of the original C-scan map of samples A–D.

4. Conclusions

Conventional eddy current inspection was performed in samples composed by carbon steel substrates coated with anticorrosive composites commonly applied inside petrochemical storage tanks. Undercoating defects, simulating localized corrosion, were detected by inspecting the same side of the machined defects. The diameters of the defects, in the range of few mm, suggest that ECT can detect corrosion at the first stages of the damages. Accuracy of the method was neither influenced by coatings thickness in the range of approx. 300–1000 μm, nor by the presence of corrosion product. The multilevel threshold processing improved the defects detectability, eliminating false defects, which usually appear as consequence of thickness heterogeneities inherent to the coatings application.

Conflicts of interest

The authors declare no conflicts of interest.

Acknowledgments

The authors would like to thank to CNPq, CAPES, FINEP and FAPERJ for the financial support and Petrobras for technical and financial assistance for the development of this study.

REFERENCES

[1] Sørensen PA, Kiil S, Dam-Johansen K, Weinell CE. Anticorrosive coatings: a review. J Coatings Technol Res 2009;6:135–76, http://dx.doi.org/10.1007/s11998-008-9144-2.
[2] Margarit-Mattos ICP, Agura FAR, Silva CG, Souza WA, Quintela JP, Solymossy V. Electrochemical impedance aiding the selection of organic coatings for very aggressive conditions. Prog Org Coatings 2014;77:2012–23, http://dx.doi.org/10.1016/j.porgcoat.2014.04.006.
[3] Margarit-Mattos ICP, Silva TC, Nascimento AV. Susceptibility to thermal aging of anticorrosive composite coating. In: 10th coatings sci int, Noordwijk. 2014.
[4] García-Martín J, Gómez-Gil J, Vázquez-Sánchez E. Non-destructive techniques based on eddy current testing. Sensors 2011;11:2525–65.
[5] Ramos HG, Ribeiro AL. Present and future impact of magnetic sensors in NDE. Proc Eng 2014;86:406–19.
[6] Udpa SS, Moore PO. Nondestructive testing handbook: electromagnetic testing. 3rd ed. American Society for Nondestructive Testing, ASNT; 2005.
[7] Mook G, Hesse O, Uchanin V. Depths penetrating eddy currents and probes. Mater Test 2007;49:258–64, http://dx.doi.org/10.3139/120.100810.
[8] Papaelias M, Cheng L, Kogia M, Mohimi A, Kappatos V, Selcuk C, et al. Inspection and structural health monitoring techniques for concentrated solar power plants. Renew Energy 2016;85:1178–91, http://dx.doi.org/10.1016/j.renene.2015.07.090.
[9] Scottini R, Quakkelsteijn HJ. Monitoring Average Wall Thickness of insulated or difficult to access objects with Pulsed Eddy Currrent. RTD Gr 2003:1–7 (PEC-2003-2).
[10] Lopes Ribeiro A, Alegria F, Postolache OA, Ramos HMG. Liftoff correction based on the spatial spectral behavior of eddy-current images. IEEE Trans Instrum Meas 2010;59:1362–7, http://dx.doi.org/10.1109/TIM. 2010.2043981.
[11] Mandache C, Brothers M, Lefebvre V. Time domain lift-off compensation method for eddy current testing. E-J Nondestruct Test 2005:10.
[12] Fan M, Cao B, Yang P, Li W, Tian G. Elimination of liftoff effect using a model-based method for eddy current characterization of a plate. NDT E Int 2015;74:66–71, http://dx.doi.org/10.1016/J.NDTEINT.2015.05.007.
[13] Dziczkowski L. Elimination of coil liftoff from eddy current measurements of conductivity. IEEE Trans Instrum Meas 2013;62:3301–7, http://dx.doi.org/10.1109/TIM. 2013.2272842.
[14] Crouzen P, Verweij M, Eggink C. Electromagnetic profiler for inspections of steel through corrosion product. 9th Eur conf ND 2006:1–9.
[15] Castleman KR. Digital image processing. Upper Saddle River, NJ: Prentice Hall Press; 1996.
[16] Russ JC. Segmentation and thresholding. Image Process. Handb. 3rd ed. CRC Press LLC; 1998. p. 324–39.
[17] Sahoo P, Wilkins C, Yeager J. Threshold selection using Renyi's entropy. Pattern Recognit 1997;30:71–84, http://dx.doi.org/10.1016/S0031-3203(96)00065-9.
[18] Park DG, Angani CS, Kim GD, Kim CG, Cheong YM. Evaluation of pulsed eddy current response and detection of the thickness variation in the stainless steel. IEEE Trans Magn 2009;45:3893–6, http://dx.doi.org/10.1109/TMAG. 2009.2024219.
[19] Angani CS, Park DG, Kim CG, Leela P, Kollu P, Cheong YM. The pulsed eddy current differential probe to detect a thickness variation in an insulated stainless steel. J Nondestruct Eval 2010;29:248–52, http://dx.doi.org/10.1007/s10921-010-0083-3.